Front. Optoelectron. 2020, 13(1): 35–49
https://doi.org/10.1007/s12200-019-0946-x

REVIEW ARTICLE

Research development on fabrication and optical properties of nonlinear photonic crystals

Huangjia LI, Boqin MA (✉)

School of Data Science and Media Intelligence, Communication University of China, Beijing 100024, China

Abstract Since the lasers at fixed wavelengths are unable to meet the requirements of the development of modern science and technology, nonlinear optics is significant for overcoming the obstacle. Investigation on frequency conversion in ferroelectric nonlinear photonic crystals with different superlattices has been being one of the popular research directions in this field. In this paper, some mature fabrication methods of nonlinear photonic crystals are concluded, for example, the electric poling method at room temperature and the femtosecond direct laser writing technique. Then the development of nonlinear photonic crystals with one-dimensional, two-dimensional and three-dimensional superlattices which are used in quasi-phase matching and nonlinear diffraction harmonic generation is introduced. In the meantime, several creative applications of nonlinear photonic crystals are summarized, showing the great value of them in an extensive practical area, such as communication, detection, imaging, and so on.

Keywords quasi-phase matching (QPM), nonlinear diffraction (ND), superlattice, nonlinear photonic crystal (NPC), reciprocal lattice vector (RLV)

1 Introduction

Nonlinear frequency conversion technology is an important branch in the field of nonlinear optics. Since the laser wavelength is determined by the energy levels of atoms, molecules or ions in the gain medium, the emitted laser cannot be at any wavelength. So the frequency conversion is performed to widen the wavelength and exploit the application of laser, which is also the development tendency of laser technology. It is necessary to satisfy the phase-matching condition for efficient nonlinear frequency conversion. The traditional birefringent phase matching (BPM) scheme has many strict requirements which greatly limit the flexibility of this technology. The quasi-phase matching (QPM) theory [1] proposed by J. A. Armstrong et al. in 1962 has more advantages than BPM. To compensate for the phase mismatch in the frequency conversion process to obtain a continuously enhanced effect, the sign of nonlinear susceptibility is changed by periodically modulating the spontaneously poled directions of the domains in this scheme. However, QPM theory could not be verified experimentally due to the limitations of crystal fabrication methods at the time. In the 1990s, M. Yamada et al. first fabricated a one-dimensional (1D) QPM crystal with periodic ferroelectric domain inversion at room temperature by means of external electric field poling method [2], which enables the rapid development of QPM technology. Researchers from Nanjing University not only fabricated crystals with 1D Fibonacci quasi-periodic structure using the electric poling method, but also performed QPM second and third harmonics generation [3,4]. Because the 1D structure can only provide with reciprocal lattice vectors (RLVs) for compensating the phase mismatch in a single direction, Berger generalized QPM theory to be used in two-dimensional (2D) structure and proposed the concept of nonlinear photonic crystal (NPC) (also known as dielectric superlattice) in 1998. Unlike ordinary photonic crystal with periodic linear susceptibility $\chi^{(1)}$, the linear $\chi^{(1)}$ of NPC is a space-independent dielectric constant, the second-order nonlinear susceptibility $\chi^{(2)}$ varies periodically in space [5]. Broderick et al. experimentally realized the generation of second and higher harmonics with 2D hexagonal superlattice [6], which indicates that the exploration and research of superlattice have gone into a new stage. In the following ten years, 2D quasi-periodic and aperiodic superlattices have been proposed so as to broaden the wavelength tuning range of nonlinear frequency conversion. Besides, the study of three-dimensional (3D) super-

Received June 15, 2019; accepted August 29, 2019

E-mail: maboqin@cuc.edu.cn

lattices has also become one of the most popular research directions in the moment.

In recent years, the researches on nonlinear diffraction (ND) harmonic generation have been highly concerned at home and abroad. The concept of ND was put forward in the 1970s, which concludes nonlinear Čerenkov radiation (NCR), nonlinear Raman-Nath diffraction (NRND) and nonlinear Bragg diffraction (NBD). There are different phase-matching conditions under these non-collinear processes. On account of the tolerance of the phase-matching condition, ND can be realized without specially designed crystal. However, various output patterns can be generated according to different superlattices of the crystal, which are potentially applied to develop new types of light source. In 2004, A. Fragemann et al. first observed the nonlinear Čerenkov second harmonic generation (CSHG) phenomena in a 1D periodic bulk NPC [7], which are highly dependent on the domain boundary and cannot be realized in a single domain crystal. Since then, NPCs with a variety of superlattices have begun to be studied in the field of ND. Saltiel's team observed the SHG of both NCR and NRND in 2D periodically poled $LiNbO_3$ [8]. Koynov et al. implemented CSHG using a 2D decagonal quasi-periodic superlattice, and pointed out it can be utilized to the visualization of ferroelectric domain [9], which provides a new way for the inspection of poling quality. The study on ND in 2D radial superlattice was proposed by researchers who pumped two collinear incident lights to interact in the crystal, eventually producing colorful Čerenkov rings [10]. After that, 2D structures of the Sierpinski fractal, sunflower spiral and so on have been come up with to be researched on ND, and they have been proved to benefit in different applications [11–13]. Today, lasers have an indispensable position in the life of modern humans. The flexible and controllable technology of frequency conversion based on NPC has opened a new stage for the fields of communication, detection, remote sensing, imaging, etc., which require lasers with higher energy and wider frequency range, and has also become one of the most powerful impetuses for the development of laser technology.

2 Fabrication of nonlinear photonic crystals

The birth of the electric field poling method at room temperature is a milestone in the field of NPC. It is currently the most commonly used method for the fabrication of 1D and 2D NPCs. The principle of this method is to force the electric dipole moment in the ferroelectric crystal to reverse by applying a pulsed high-voltage electric field that is stronger than the internal coercive electric field of the crystal, so that the direction of spontaneous nonlinear susceptibility varies along with the formation of inverted domains in the crystal. In practice, the electric field poling method at room temperature is usually combined with the semiconductor processing technology. First of all, the mask is specially designed with the same structure as the superlattice. Secondly, the photoresist spin-coated on the surface of the crystal is partially removed using the pre-designed mask by photolithography. Then the surface of the crystal without photoresist is exposed in electrolyte [14] or installed with Al films [2] to form electrodes, as shown in Figs. 1(a) and 1(b), respectively. Finally, a suitable pulsed electric field is applied for poling. The applied voltage is usually set as 25 kV/mm and the poling depth is about 400 μm. The technique can fabricate NPCs with uniform inverted domains at room temperature, has high controllability of duty cycle, and is easy for manufacturing in commercialization. For many other specific circumstances such as periodically poled $LiNbO_3$ waveguides, surface poling and short-pitch poling, there are also different methods including chemical indiffusion, scanning force microscopic poling, electron-beam poling, probe-tip poling and the crystal-growing technique [16–20].

However, the nonlinear susceptibility along the optical axis cannot be modulated by all of the methods mentioned

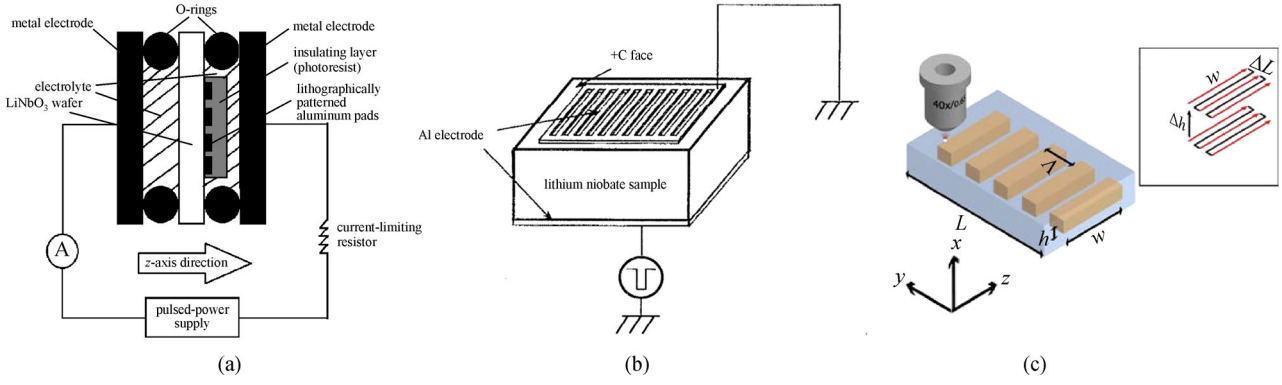

Fig. 1 Experimental schematic of fabrication methods of nonlinear photonic crystals. (a) Electric field poling method with electrolyte; (b) electric field poling method with Al electrode [2]; (c) femtosecond direct laser writing technique [15]. The inset outlines the inscription routine in which the black lines indicate the switch of the laser is turned off

above, resulting in the missing of RLVs in this direction. In other words, the modulation is limited to 2D superlattices. It is demonstrated that the phase matching can be realized just by periodically modulating the magnitude of the nonlinear susceptibility rather than reversing the sign of it. And the conversion efficiency depends on how strongly the nonlinear susceptibility is affected by the modulation, which is also known as the modulation depth. For example, the periodic domain inversion superlattices with the largest modulation depth has higher nonlinear conversion efficiency than those with damping domain. Therefore, in some cases where it is difficult to realize domain poling, we can reduce the nonlinearity of the medium. The researchers proposed the femtosecond direct laser writing technique based on the above principle [21]. Using a microscope objective to focus a femtosecond pulsed laser with suitable energy on the surface or inside of the crystal, the nonlinear susceptibility at the focal spot is significantly reduced [15], as shown in Fig. 1(c). In contrast to the electric poling method, the femtosecond direct laser writing technique enables three-dimensionally modulation of nonlinearity including the optical axis direction. In addition, a series of lithographic processes such as making patterned mask are eliminated, which reduces the complexity of the fabrication process. Whereas, it has a higher time cost in the fabrication of large-area superlattices.

3 Quasi-phase matching and nonlinear diffraction harmonic generation

The realization of QPM is based on both energy and momentum conservation. Taking the SHG as an example, the phase-matching relationship is $\Delta\vec{k} = \vec{k}_{2w} - 2\vec{k}_{w} - \vec{G}_m$, where $\vec{k}_{2w}$ is the second harmonic (SH) wave vector, $\vec{k}_{w}$ is the fundamental wave (FW) vector, and $\vec{G}_m$ is the RLV in NPC. The QPM will be completely achieved when the phase mismatch $\Delta\vec{k}$ resulted from the dispersion of crystals is fully compensated by the involved RLV. According to the formula $G_m = \dfrac{2\pi m}{a+b}$, it is obvious that the RLVs are related to the period $\Lambda = a + b$ of NPCs, where a and b are the widths of positive and negative domains, respectively, and m indicates the order of RLV. Therefore, the QPM harmonic processes of different wavelengths and directions can be realized by adjusting the period of the NPCs or their RLVs [22]. As shown in Fig. 2(a), although QPM is not as efficient as BPM, its flexible implementation and less requirements for crystals bring it to the fore in the field of frequency conversion. To achieve the tunability of continuous output wavelengths and enable the energy of them to meet practical application requirements, one essential step is to design and fabricate different domain inversion periods in NPCs. As a result, the QPM technology has been increasingly favored nowadays.

The NCR of ND is an extension from Čerenkov radiation in the field of high energy particle physics to the field of nonlinear optics, which can be spontaneously generated at the interface of two media such as domain wall or crystal boundary without RLVs compensation. As shown in Fig. 2(b), the longitudinal phase-matching condition $|2\vec{k}_{w}| = |\vec{k}_{2w}|\cos\theta_c$, where θ_c is the Čerenkov radiation angle between the propagation directions of FW and SH, is automatically satisfied. So the radius of the Čerenkov ring is independent of the superlattice. Compared to this, the NRND generated by the diffraction effects among the second harmonics emerged from different domain walls satisfies the transverse phase-matching condition $|\vec{G}_w| = |\vec{k}_{2w}|\sin\beta$, as shown in Fig. 2(c). So the distribution as well as the position of the NRND pattern are highly correlated with the superlattice. Unlike NCR and NRND with partial phase matching, the NBD meets both transverse and longitudinal phase-matching conditions, as shown in Fig. 2(d). When the radiation angle of NCR is equal to the one of NRND ($\theta_c = \beta$), the two ND processes occur simultaneously, which generates the NBD. However, the occurrence of NBD is restricted to certain parameters of the NPC, the operating wavelengths, and the incidence angles of the fundamental beam [23–26].

4 Development of various superlattice structures

4.1 One-dimensional superlattices

In 1997, Fejer et al. performed the SHG experiment pumped by a single-pass continuous wave (CW) 1.064-μm Nd:YAG on a periodically poled lithium niobate (PPLN), and the frequency conversion efficiency is up to 42% [27]. Subsequently, some researchers used this single-period superlattice to explore the ND phenomenon, and obtained multi-order ND double-frequency output, which is distributed regularly on the screen. As shown in Figs. 3(a) and 3(b), the central diffraction spots grouped around the pump position are nonlinear optical analogs of Raman-Nath diffraction, while the peripheral diffraction spots situated symmetrically far from the pump at both sides of the diffraction array are resulted from NCR [28]. Recently, Chen et al. suggested to modulate the phase of FW with a spatial light modulator, termed as structured fundamental wave (shown in Fig. 3(c)), to substitute the structured NPC in NRND harmonic generation [29]. The results of the experiment on 1D periodically modulated FW are shown in Fig. 3(d), where the multi-order NRND frequency-

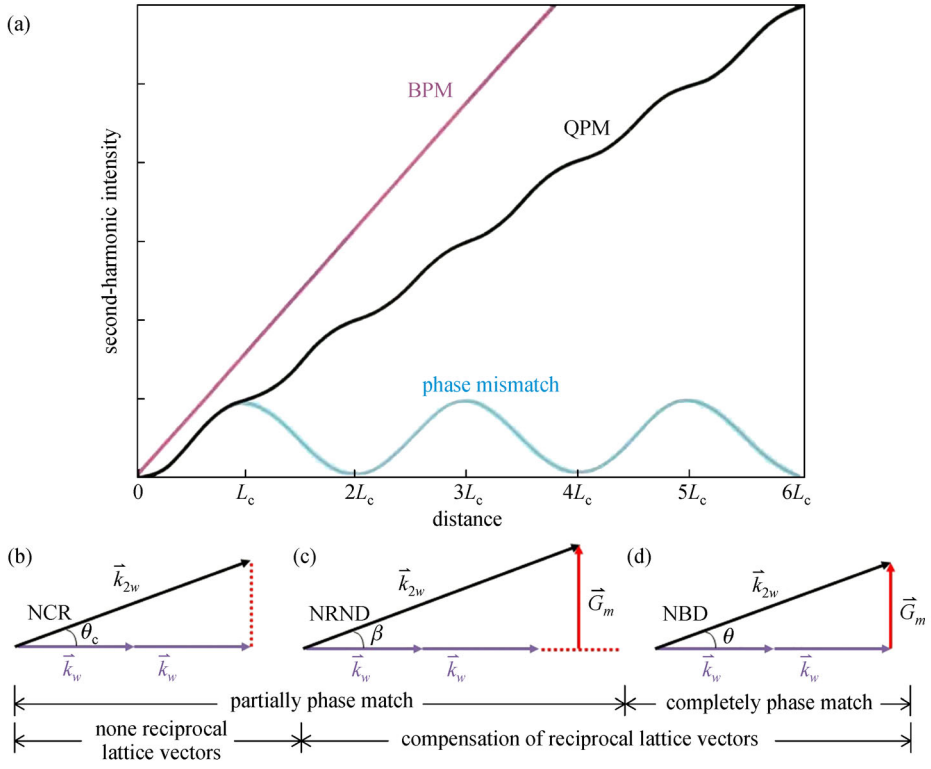

Fig. 2 All the types of phase-matching condition during $\chi^{(2)}$ processes. (a) Birefringent phase matching (BPM) and quasi-phase matching (QPM) processes [22][1)]; (b) spontaneously longitudinal phase matching generates nonlinear Čerenkov radiation (NCR) without reciprocal vectors compensation; (c) transverse phase matching compensated by reciprocal vectors generates nonlinear Raman-Nath diffraction (NRND); (d) nonlinear Bragg diffraction (NBD) generated by both transverse and longitudinal phase matching

doubling light is clearly visible and basically consistent with the results obtained by the traditional NRND experiment. However, the 1D single-period superlattices can only provide effective RLVs in one direction to compensate the phase mismatch in the nonlinear interactions, which makes the frequency conversion only be applied to a specific wavelength and cannot be discretionarily selected.

Inspired by the quasicrystal structure, Ming et al. proposed a 1D Fibonacci optical superlattic (FOS). Unlike single-period superlattice with the first-order RLV only in one direction, the new superlattice structure can provide high-order RLVs to meet different phase-matching requirements [3]. The FOS includes two kinds of basic blocks A and B with different periods. In A and B, there are positive domains of the same widths $l_{A1} = l_{B1} = l$, and negative domains of different widths $l_{A2} = l(1+\eta)$ and $l_{B2} = l(1-\tau\eta)$ respectively, where l, η are adjustable structure parameters, τ is the golden ratio. Blocks A and B are arranged according to the production rule of Fibonacci sequence $S_j = S_{j-1}|S_{j-2}$, $j \geqslant 3$ and $S_1 = A$, $S_2 = \mathrm{AB}$, as shown in Fig. 4(a). With FOS, they not only implemented SHG of multiple wavelengths, but also coupled SHG with sum frequency generation (SFG) process to directly achieve third harmonic generation (THG). Afterwards, they designed a 1D cascaded optical superlattice consisting of two different structures in series in the same $LiTaO_3$ crystal wafer. The first one is a dual-periodic structure, which can be described as a periodic phase-reversal sequence superimposed upon another smaller periodic structure, as shown in Fig. 4(b). The second one is configured with seven parallel channels, each 1 mm in width, but with different periods, which are incremented by a step of 0.005 μm in the range of 4.85 to 4.89 μm. These seven channels correspond to seven different phase-matching temperatures for the generation of blue light. By simultaneous SHG and THG within the superlattice, the red, green and blue lights are generated at the same position with a certain proportion of intensity, leading to the synthesis of a quasi-continuous, quasi-white-light laser [30]. Moreover, Li's research team proposed the chirped periodically poled lithium niobate (CPPLN) to simultaneously achieve the high-efficiency broadband high-order QPM SHG and THG [31]. In the chirped superlattice, the widths of negative domains are fixed, while the widths of positive domains gradually decrement along the light-

1) Reproduced from Ref. [22], with the permission of the American Institute of Physics

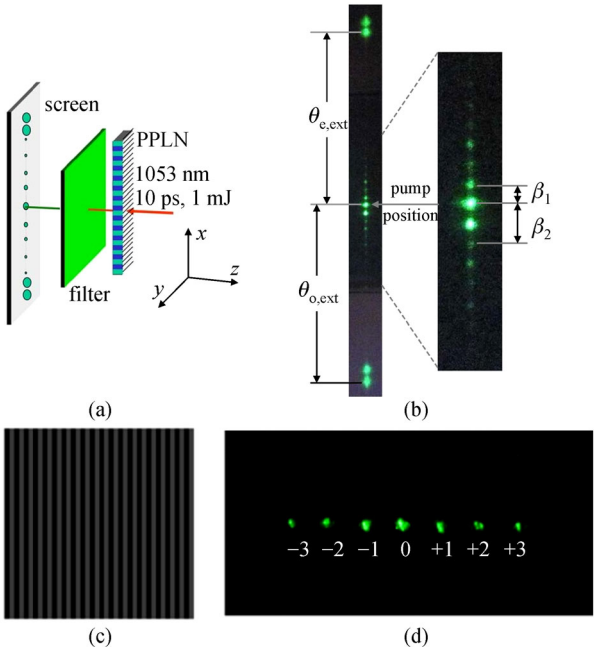

Fig. 3 Experimental schematic and observed second harmonic diffraction patterns of nonlinear Raman-Nath diffraction in one-dimensional single-period structure. (a) Experimental schematic with structured nonlinear photonic crystal [28][1)]; (b) nonlinear diffraction pattern of structured nonlinear photonic crystal [28]; (c) holograms loaded on spatial light modulator representing the phase structure of the fundamental wave [29][2)]; (d) nonlinear diffraction pattern of structured fundamental wave [29]

propagation direction, as shown in Fig. 4(c). As a result, continuously varying RLVs can be generated to compensate phase mismatch. Mutually verified by theory and experiment, it is concluded that the bandwidth widens but the conversion efficiency decreases as the chirp rate increases. The 1D short-range ordered superlattice proposed by Wang et al. is alternately composed of periodically poled ferroelectric segments with certain width and random extended single domain, which is a combination of periodicity and disorder, as shown in Fig. 4(d). It is demonstrated that the conversion efficiency of SHG in this superlattice can be improved by increasing the length of the crystal, while the spectral bandwidth can be controlled by the total length of periodically poled ferroelectric segments [32].

The experimental parameters and results of QPM nonlinear frequency conversion based on various one-dimensional superlattices are shown in Table 1. It can be seen that the conversion efficiency of single-period superlattice is the highest, although the frequency conversion for only one wavelength is realized. Both of the FOS and CPPLN can carry out the frequency conversion of multiple wavelengths, but QPM SHG within the latter is implemented in 4 wavebands from 0.85 to 1.48 μm, and a wider bandwidth can be achieved than the corresponding waveband of the former. Besides of this, the THG process of CPPLN can also be performed in a continuous waveband, but is not as efficient as FOS. A broadband output can be achieved within short-range ordered superlattice on account of its high rate of disorder, whereas the conversion efficiency is very low. In summary, the conversion efficiency and bandwidth are two mutually restricted performance parameters. By the optimization of different superlattices, a certain balance between the two parameters can be achieved to meet the requirements of different applications.

In addition to the superlattices above studied by experiment, Gu et al. theoretically studied the 1D aperiodic optical superlattice (AOS), which is divided into many blocks with alternate domain inversion. The construction of AOS depends on the specified nonlinear optical process, and the widths of blocks are not necessarily equal to each other, but must be an integer multiple of a basic width. For instance, since the conversion efficiency of SHG process is positively correlated with the effective nonlinear coefficient ξ_{eff}, which is strongly dependent on the configuration of domains as well as the phase lagging from one block to the other block, it is evident that the optimization construction of the AOS for the SHG can be ascribed as a search for the maximum of ξ_{eff}. Such an optimization nonlinear problem can be solved with the simulated annealing method and then the favorable arrangement of

1) Adapted with permission from Ref. [28], © The Optical Society
2) Adapted with permission from Ref. [29], © The Optical Society

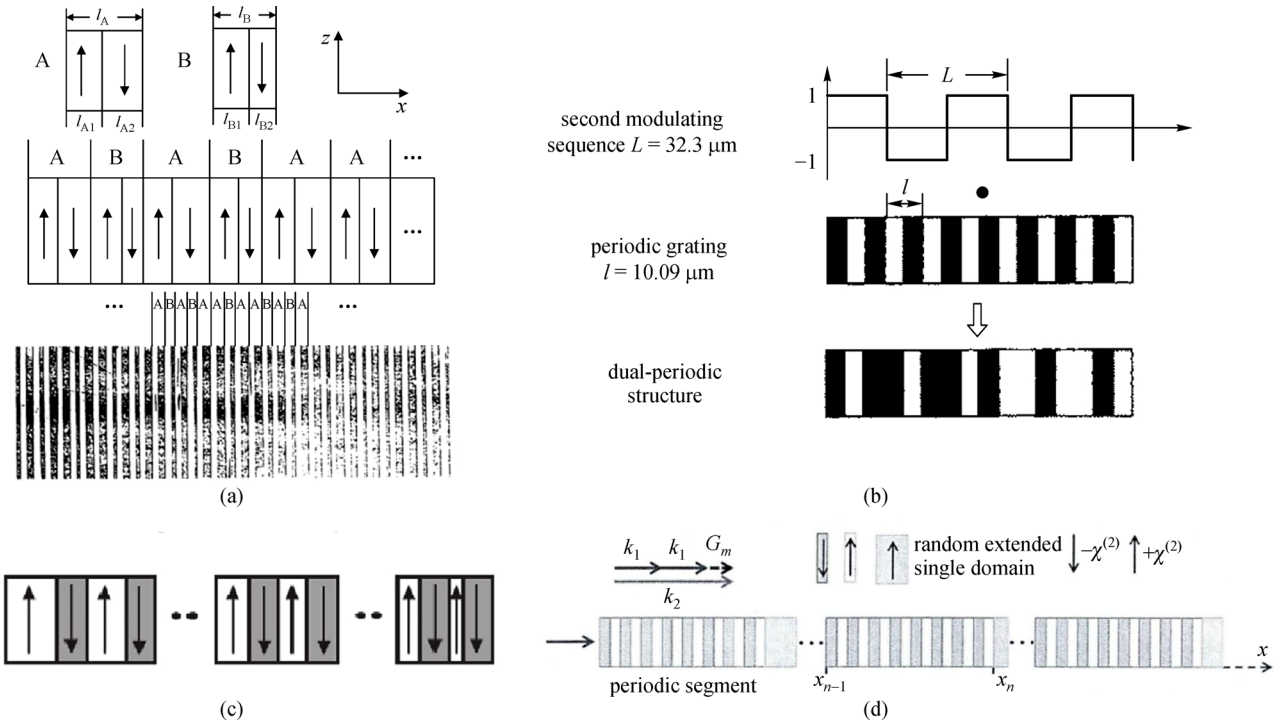

Fig. 4 Schematic diagrams of the structural geometry in one-dimensional superlattices. (a) Fibonacci quasi-periodic superlattice [3]; (b) cascaded dual-periodic superlattice [30]; (c) chirped superlattice [31]; (d) short-range ordered superlattice [32]

Table 1 Experimental parameters of quasi-phase matching harmonic generation in one-dimensional superlattices

Ref.	superlattice structure	ferroelectric crystal	fundamental wavelength/μm	nonlinear effect	harmonic wavelength/μm	conversion efficiency	bandwith /nm
[3]	Fibonacci	$LiTaO_3$	0.9726, 1.0846, 1.2834, 1.3650, 1.5699	SHG	0.4863, 0.5423, 0.6417, 0.6825, 0.7845	7.5%, 17.5%, 9.1%, 6.7%, 20.4%	0.3, 0.4, 0.85, 1.1, 2.5
		$LiTaO_3$	1.570	THG	0.523	23%	5
[27]	single-period	$LiNbO_3$	1.064	SHG	0.532	42%	–
[30]	cascaded (dual-period + 7 channels)	$LiTaO_3$	1.064, 1.342	SHG + THG	447, 532, 671 quasi-white-light	3%	–
[31]	chirped	$LiNbO_3$	1.37 – 1.47	SHG	0.69 – 0.74	30%	98
		$LiNbO_3$	1.38 – 1.45	THG	0.46 – 0.48	2%	74
[32]	short-range ordered	$LiNbO_3$	1.50	SHG	0.75	0.23%	60

Notes: SHG: second harmonic generation; THG: third harmonic generation

the domain orientations of the blocks in the sample can be determined completely [33]. Simulating SHG and THG processes in AOS based on $LiTaO_3$ crystal, they achieved multi-wavelength conversion with higher efficiency than that in FOS.

Based on the mature theory of NPC, Segal et al. unprecedentedly demonstrated control over the nonlinear harmonic generation from metamaterials by constructing the first nonlinear metamaterial-based PCs [34]. These metamaterials are made as an arrangement of artificial structural resonant elements, which are usually on the nanoscale. Integrating the small size of metamaterials into the ability of NPCs to control nonlinear interactions, there are broad development prospects in the nonlinear metamaterial-based PCs for ultra-compact nonlinear optical devices. They chose tightly packed groove-like split-ring resonators to be the metamaterials and all-optically manipulated the direction of the second harmonic from a 1D periodic nonlinear metamaterial-based PC. Besides, they also designed a nonlinear metamaterial-based PC that acts as a nonlinear binary-phase Fresnel zone plate to directly focus the nonlinear emission. After that, other

researchers proposed the 1D quasi-periodic metamaterial superlattices, such as Cantor-like, Thue-Morse-like and Fibonacci-like [35,36]. And they demonstrated large enhancement efficiencies and broadband applicability for SHG with these metamaterial superlattices. Gómez et al. concentrated on defective metamaterial photonic superlattices, which composed by alternating layers of conventional dielectric and negative refractive material slabs with a dielectric defective layer [37–39]. They reported the existence of multiple omnidirectional defect modes, analyzed the tunable parameters and found out its ability to greatly enhance the second harmonic conversion efficiency.

4.2 Two-dimensional superlattices

The RLV of 2D NPC is represented by $\vec{G}_{m,n}$, which differs from $\vec{G}_m$ in the ordinary 1D NPC. The RLVs of the same order in 2D NPC distribute in multiple directions such as the first-order $\vec{G}_1$ of 1D NPC and $\vec{G}_{0,1}$, $\vec{G}_{1,0}$ in different directions of 2D NPC. The 2D RLV indexing comes from the fact that the 1D quasi-periodic superlattice is nothing but the projection of a 2D periodic crystal on a 1D axis [5].

Hexagonal NPC is the first 2D superlattice used in experiments, as shown in Fig. 5(a). Broderick et al. at Southampton University first prepared a $LiNbO_3$ NPC with hexagonal superlattice in 2000, not only carrying out QPM SHG with conversion efficiency greater than 60%, but also generating green and blue light outputs [6]. Ming et al. experimented on a hexagonally poled waveguide to generate NCR. Unlike most ND experiments in which the incident light propagates along z-axis, the two z-polarized FWs at 1.064 and 1.319 μm were collinearly coupled into the waveguide by a cylindrical lens transmitting along the x-axis of the crystal in their scheme. Finally, the multi-order QPM and NCR SHG patterns composed of red, green and yellow spots and lines, which is just like a

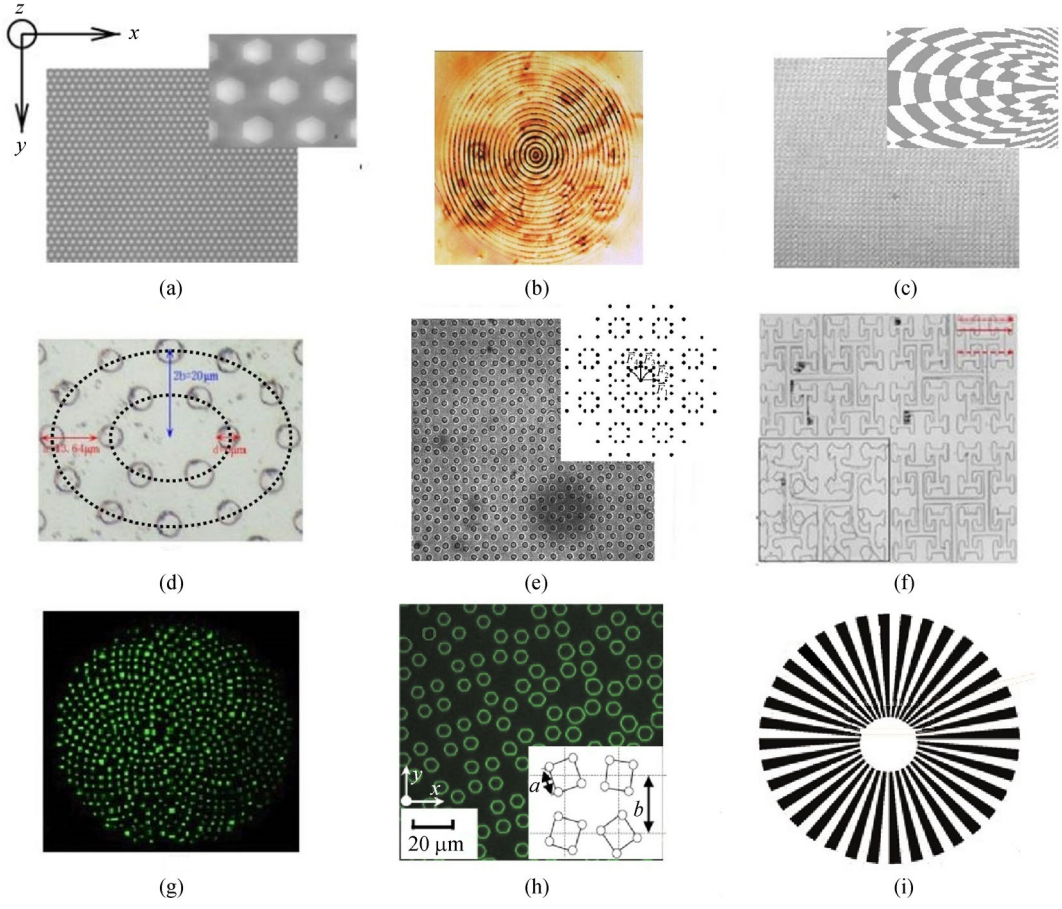

Fig. 5 Schematic diagrams of the structural geometry in two-dimensional superlattices. (a) Hexagonal superlattice [6]; (b) annular superlattice [40][1]; (c) brick-like superlattice [41]; (d) ellipse superlattice [42]; (e) octagonal superlattice [43]; (f) H-fractal superlattice [44]; (g) sunflower spiral superlattice [12][2]; (h) short-range ordered superlattice [13]; (i) radial superlattice [10]

1) Adapted with permission from Ref. [40], © The Optical Society
2) Adapted with permission from Ref. [12], © The Optical Society

"Christmas tree," was projected on the screen [45]. The square superlattice is also one of the most basic 2D periodic structures, with which many researchers have implemented QPM and ND effects focusing on different performances. Zhang's research team took the lead in QPM SHG experiment and obtained 42% conversion efficiency [46]. Then Peng et al. realized multi-wavelength tunable SHG with it, obtaining a bandwidth up to 150 nm at sample rotation angle of −8 degrees [47]. Since then, rectangular NPC has also been demonstrated to enable high efficiency multi-wavelength QPM and ND harmonic generation [48,49]. As shown in Fig. 5(b), the 2D annular NPC with continuous rotational symmetry but no translational symmetry consists of a series of concentric rings of the same period, so the incident angle does not affect the QPM process when the pump passes exactly at the center of the structure [40,50]. The annular NPCs with different periods fabricated by indirect e-beam method and electric field poling method were used in experiments, showing that several harmonics involving multi-order RLVs can be presented simultaneously at different angles. Extending the Huygens-Fresnel principle to nonlinear optical parametric processes, Zhu et al. specially designed two new superlattices to combine three optical functions: generation, focusing and beam splitting of SH, which opens a door for compact devices [41]. As shown in Fig. 5(c), the proposed brick-like structure with neither translational symmetry nor annular symmetry is able to convert a weakly focused FW with a beam waist of 300 μm into two tightly focused SHs with a beam waist of 120 μm, which are symmetrically distributed on the two sides of the FW. The other periodic-like one can realize single focused SHG with the focused points located 10 cm away from the exit surface and 42% conversion efficiency. For dual focused SHG mentioned above, the two focused points are 2 mm apart with 24% conversion efficiency. The 2D ellipse superlattice proposed by Li et al. in 2014 comprises with quantities of concentric elliptical rings, and the ith elliptical ring is composed of $6i$ fixed-size circular negative domains, which provides continuously varying RLVs in different directions [42], as shown in Fig. 5(d). The experimental data show that this structure can realize broadband QPM SHG with the highest efficiency of 46.8% in multiple incident directions in the range of $0-90$ degrees under pump deletion.

Our research team proposed a 2D octagonal quasi-periodic superlattice, as shown in Fig. 5(e). It is unique with octagonal rotational symmetry, and the QPM process can still be achieved when the crystal is rotated by an integer multiple of $\pi/4$ around the z-axis. Different from the RLVs in 2D periodic superlattice, the RLVs of 2D quasi-periodic superlattice need to be represented by four integer indexings as $\vec{G}_{m,n,p,q}$, that is to say, all of the RLVs of it are linear combinations of the four basis vectors: $\vec{F}_1 = (1000)$, $\vec{F}_2 = (0100)$, $\vec{F}_3 = (0010)$, $\vec{F}_4 = (0001)$. With the octagonal structure, not only a high-efficiency collinear QPM SHG is realized, but also non-collinear QPM SHG with FW ranging from 0.882 to 1.363 μm are obtained in the same incident direction, and the SH spots are symmetrically distributed at both sides of the FW [43]. Moreover, the decagonal quasi-periodic superlattice has basis vectors in five directions because of its decagonal rotational symmetry. Similarly, the QPM process is still available when the crystal is rotated by an integer multiple of $\pi/5$ around the z-axis with an abundant distribution of $\vec{G}_{m,n,p,q,r}$. Sheng et al. achieved quasi-continuous multi-wavelength collinear SHG in such a superlattice basing on the principle to use the projections of RLVs onto the direction of propagation to satisfy phase-matching condition. The projection-based QPM makes the best use of RLVs in the superlattice, obtaining a maximum conversion efficiency of 34% [51]. Theoretically, the higher the level of symmetry of the quasi-periodic structure is, the more abundant the distribution of RLVs is. However, when the quasi-crystal symmetry is enhanced, the adjacent inverted domains with minor period are likely to be connected into one due to the spontaneous lateral expansion of the domain wall with external electric field poling method. If there is a NPC with relatively sparse arrangement of superlattice and abundant RLVs, it will be possible to obtain more efficient nonlinear effects following the traditional electric field poling method. So it remains an urgent task to explore other superlattices.

The fractal is a self-similar structure with many substructures which can be seen as scaling and translation transformations of the initial fractal unit, as shown in Fig. 5(f). There are several different inverted domains distributed at different longitudinal positions along the y-axis, leading to differences in the distribution of RLVs. Wen et al. theoretically analyzed the H-fractal optical grating and pointed out that its diffraction pattern also exhibited self-similarity [52]. Due to the coherent superposition of the lights diffracted of different levels of substructures in this grating, the total output is more intense at high frequencies than at low frequencies. And it is shown that the diffracted spots become brighter when moving away from the center of the pattern, which is in stark contrast to those obtained from ordinary 1D and 2D gratings. Benefiting from this character, the superiority of H-fractal grating for high-order diffraction process is revealed. It is also worth noting that this diffracted light intensity distribution character is desirable because of enhanced intensity of diffraction orders at large diffraction angle, which can lead to improved dispersion capacity. As the H-fractal grating is introduced into NPC, the QPM SHG process is carried out with a flexible tuning range, showing that multi-wavelength harmonic generation requiring different RLVs at different positions can be realized at the same time [44]. Chowdhury et al. implemented the 11th harmonic generation in mid-infrared region with a $LiNbO_3$ of Sierpinski carpet fractal super-

lattice, reaching a conversion efficiency of 13% cumulated from all harmonics, which is significant for the generation of femtosecond ultraviolet pulses [53]. In addition, there have been related studies on aspect of ND in the Sierpinski fractal superlattice, and harmonic waves up to the 4th order have been generated [54]. It is concluded by theoretical analysis that different orders of NCR or NBD harmonics with the same radiation angle originated from multi-wavelength FWs can be superimposed at the same position, while different orders of them with different colors generated from single wavelength FWs appear at different positions. Similarly, Spanish researchers used the two-dimensional square superlattice to obtain simultaneous generation of 2nd to 5th harmonics [55]. Recently, a new type of superlattice named sunflower spiral (also known as golden-angle spirals) has been proposed by Australian researchers to enhance CSHG, as shown in Fig. 5(g). Instead of being poled by electric field, the high-quality and small-period $LiNbO_3$ samples with sunflower superlattice were fabricated by femtosecond laser direct writing technique. As shown in the diffraction pattern, the sunflower superlattice offer a diffusive, circularly symmetric distribution of RLVs compared with the narrow discrete distribution of those in the ordinary annular superlattice [12].

Because of the diverse RLVs directions in 2D superlattice, most of them are used to carry out multi-wavelength harmonic generation, as shown in Fig. 6. The square and rectangular periodic superlattices with the highest overall conversion efficiency are measured under a few fundamental wavelengths, which is inferior to the fractal and quasi-periodic superlattices in terms of the FW's continuity. The advantages of the fractal superlattice are more reflected in the high-order frequency conversion, while the performance of the quasi-periodic superlattice is balanced with both of high conversion efficiency for some wavebands and wide range of operating wavelengths. Although the harmonic generation involved in multi-directional high-order RLVs is not as efficient as that in 1D superlattices, these 2D superlattices have more flexibilities as well as less restrictions on the propagation directions of FW and SH.

The exploration of ND has also led to many novel superlattices and experimental schemes as below. The researchers studied CSHG process of the sunflower superlattice, producing a clear double-ring harmonic output under the fundamental wavelength range of 1.2 – 1.6 μm [12]. The observed far-field harmonic pattern is shown in Fig. 7(a), where the external ring is the Čerenkov second harmonic and the internal ring is the Raman-Nath second harmonic. When the fundamental wavelength is 1.3 μm, the transverse and longitudinal phase-matching conditions are simultaneously satisfied, resulting in the NBD SHG with the clearest and brightest output. This superlattice breaks down the barrier that strong NCR is confined in a specific direction in

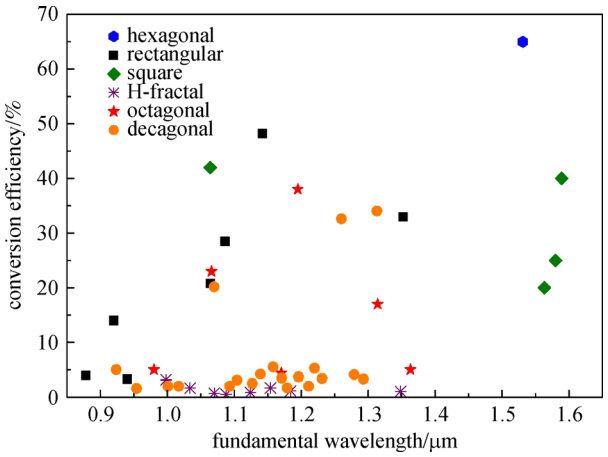

Fig. 6 Conversion efficiencies under multiple fundamental wavelengths within two-dimensional superlattices

conventional periodic and quasi-periodic superlattices, so that the broadband CSHG can be carried out at any azimuths. Besides, a 2D short-range ordered $LiNbO_3$ with partial disorder is used to implement CTHG, as shown in Fig. 5(h). When the 1.5 μm-FW is input, the second and third ring-shaped harmonics of red and green, respectively, are generated [13], as shown in Fig. 7(b). It has been found that the 2D short-range ordered superlattice is independent with the position and size of the NCR ring but enhances the intensity of it. The results of the experiments on ND process using $LiTaO_3$ with 2D rectangular and annular superlattices are also worked out [49]. Similar to the results of ND in 1D superlattices, the diffraction patterns of the superlattices are presented in the center by NRND effect. Based on the comparative analysis among the four superlattices, an important experimental observation is the two types of azimuthal modulations of the Čerenkov rings. For the first type, the 6-fold modulation of the diffraction rings comes from the hexagonal shape of the domains in $LiNbO_3$ crystal; for the second type, the azimuthal position of modulation with one maxima in $LiTaO_3$ crystal depends on the orientation of input polarization. Furthermore, Zhu et al. and Australian researchers concentrated on the ND processes in 2D radially (Fig. 5(i)) and rectangularly poled NPCs illuminated by two collinear [10] and two overlapping noncollinear [56,57] FWs, respectively. And the generated Čerenkov rings of their experiments are shown in Figs. 7(c) and 7(d), respectively. Shur et al. from Russia conducted extensive research on NBD and realized multiple intensive NBD by applying femtosecond laser pulses of specific wavelengths in a rectangular superlattice. Experiments show that when the wavelength of the femtosecond pulsed FW is 856 nm, the highest SHG conversion efficiency can be achieved and the clearest and brightest NBD blue light is observed [58].

In addition, researchers concerning on metamaterials also made progress on 2D superlattices. Segal et al.

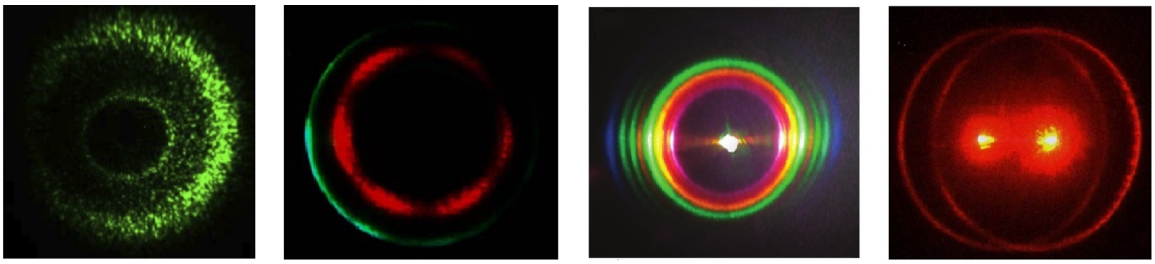

Fig. 7 Nonlinear diffraction second or third harmonic generation in two-dimensional superlattices. (a) Sunflower spiral $LiNbO_3$ [12][1]; (b) short-range ordered $LiNbO_3$ [13]; (c) two collinear fundamental waves [10]; (d) two crossed noncollinear fundamental waves [56][2]

constructed not only 1D periodic metamaterials, but also 2D periodic and quasi-periodic nonlinear metamaterial-based PCs which are triangular lattice with 6-fold symmetry, square lattice with 4-fold symmetry and Penrose lattice with 10-fold symmetry [34]. Shortly, Almeida et al. proposed a V-shaped gold nanoantenna. By adjusting the lengths of the arms and the angles between them for these antennas, the plasmonic resonance transmission intensity can be tuned. It is concluded that the resonance peak moves to longer wavelengths for longer arm length and smaller angles [59].

4.3 Three-dimensional superlattices

Compared with the RLVs of 1D superlattices in a single direction and 2D superlattices in a plane, the 3D superlattices provide with abundant RLVs in a space. In 3D NPCs, the arrangement of inverted domains can be arbitrarily designed in three dimensions, leading to the phase matching at any angle and even the omnidirectional modulation of the spatial mode and spectrum of the light wave. Taking the 3D tetragonal superlattice with a period of d as an example, there is not only the RLV with magnitude of $2\sqrt{2}\pi/d$ which also belongs to the 2D square superlattice with the same period, but also the RLV with magnitude of $2\sqrt{3}\pi/d$ in the 3D one. In 2016, researchers at Shandong University prepared a 3D $Ba_{0.77}Ca_{0.23}TiO_3$ (BCT) crystal through the Czochralski crystal growth method, and obtained petal-like SH patterns of different colors generated by QPM with the fundamental wavelength ranging from 0.9 to 1.5 μm [20]. However, it is still unable for the preparation of a scientifically-based superlattice with artificial structure.

In 2018, the journal *Nature Photonics* published two papers from Nanjing University [60] and Australian National University [61], presenting their research achievements on 3D NPCs. A 3D tetragonal superlattice was fabricated by femtosecond laser for the first time in $LiNbO_3$ crystal and BCT crystal, as shown in Figs. 8(a) and 8(b), respectively. Although the nonlinear susceptibilities $\chi^{(2)}$ are modulated by femtosecond lasers, the details of their preparation processes are quite different from each other. The former optimizes the laser parameters to selectively erase $\chi^{(2)}$ and reduces the nonlinearity of certain positions, while the latter directly inverts the ferroelectric domain at the corresponding positions by utilizing the nonlinear absorption of tightly focused infrared femtosecond laser. Obviously, the both methods achieve a breakthrough in all-optical poling of ferroelectric crystals. The frequency doubling experiments verified that there are more abundant RLVs in the 3D tetragonal superlattice, especially for the RLVs parallel to the z-axis of the crystal, which are difficult to be obtained by the conventional electric poling method. And the QPM SHG conversion efficiency is significantly enhanced in the 3D superlattice in comparison with that in the single domain crystal. The experiment with $LiNbO_3$ crystals shows high rate of phase matching for short wavelengths, obtaining high efficiency at a FW of 829 nm, which is potential for the generation of ultraviolet light sources. In addition to the experimental investigations, researchers at Shanghai Jiaotong University theoretically analyzed the nonlinear optical properties of QPM and ND in 3D NPCs [62], finding that the three wave mixing follows the similar rules of 1D and 2D NPCs under certain approximate conditions. They simulated the nonlinear effects in 3D cylindrical and cubical superlattices, and deduces how the period of superlattices make an influence on ND process. As shown in Fig. 8(c), these two superlattices are shaped like "Rubik's Cube". The domain inversion is periodically eliminated in some layers along the optical axis of the previous two 3D samples used in experiments, so there are still many positive domains projected to the x-y plane. As for the "Rubik's Cube"-shaped superlattices simulated by computer, the positive and negative domains are interlaced in the whole 3D space, leading to no positive domains projected to the x-y plane. Since the RLVs of them are more densely distributed, QPM SHG with higher efficiency is able to be obtained. If the mentioned preparation methods

1) Adapted with permission from Ref. [12], © The Optical Society
2) Adapted with permission from Ref. [56], © The Optical Society

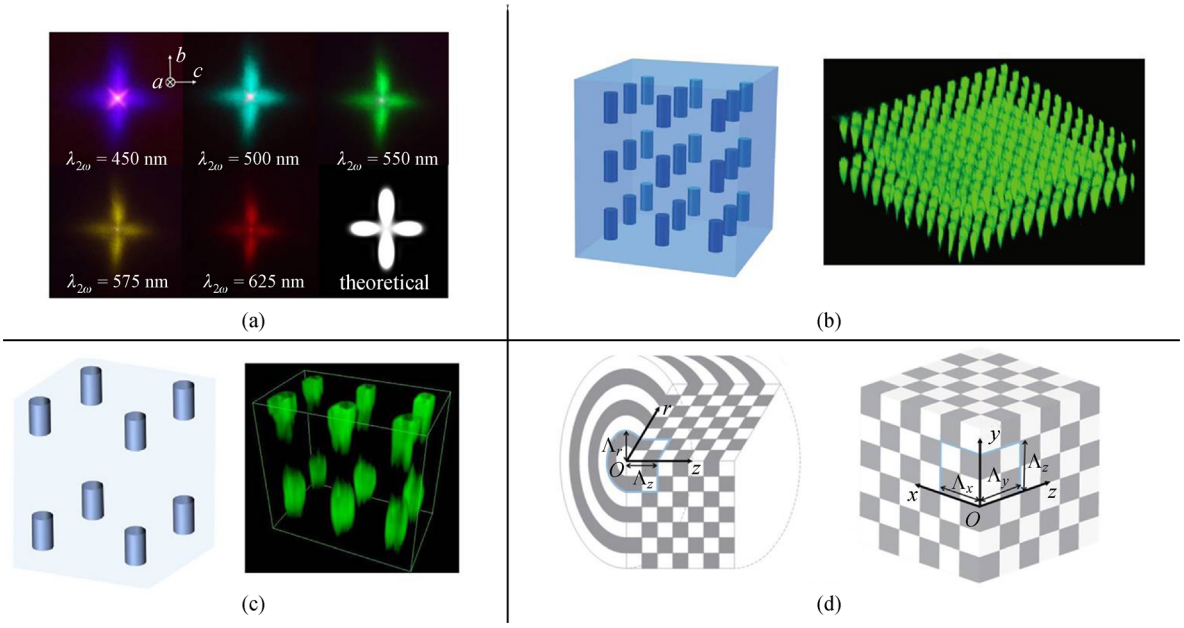

Fig. 8 Patterns of quasi-phase matching harmonics and schematic diagrams of the structural geometry in three-dimensional superlattices. (a) Patterns of harmonics generated from naturally grown $Ba_{0.77}Ca_{0.23}TiO_3$ [20]; (b) tetragonal $LiNbO_3$ fabricated by femtosecond laser engineering [60]; (c) tetragonal $Ba_{0.77}Ca_{0.23}TiO_3$ fabricated by tightly focused infrared femtosecond laser pulses [61]; (d) cylindrical and cubical structures simulated by computer [62][1)]

for 3D NPCs are used to fabricate samples of these two complex superlattices, this inference will be experimentally verified. In a word, the expansion of QPM from 2D to 3D offers more freedom and choices for NPC applications in the field of nonlinear optics and quantum optics, which will be the focus of the research on NPC in the future.

5 Applications

The ferroelectric domain visualization is one of the most common applications of NPC. The principle is the dependence of ND on the domain walls: the beam focused on the boundary of two antiparallel domains leads to CSHG emerging from the face perpendicular to the domain walls; while the beam focused on a homogeneous part of a single domain is not capable for such a nonlinear effect [9]. Therefore, the NCR harmonics emitted from the domain walls can record the morphological characteristics and distribution of the domain walls with high resolution, as shown in Fig. 9(a). Different from etching, scanning electron microscopy and atomic force microscopy, which are only suitable for the surface detection, this Cerenkov-type SHG laser scanning microscope can even produce 3D images by stacking *x*-*y* scans recorded at different depths inside the medium through adjusting the focal position of the laser along the direction of the optical axis. The birth of this method which is widely used now establishes the foundation for the study of more complex NPC structures.

The optical parametric oscillator (OPO) converts the input pump light with a wavelength of λ_p into two output lights with longer wavelengths — the signal light with a wavelength of λ_s and the idle light with a wavelength of λ_i through the second-order nonlinear interaction $\frac{1}{\lambda_p} = \frac{1}{\lambda_s} + \frac{1}{\lambda_i}$. The essence of the parametric process in OPO is the QPM difference frequency generation (DFG), which can be regarded as an inverse process of SFG. To vary the wavelengths of the output lights, the pump light and the superlattice of the QPM crystal is usually adjusted to meet the phase-matching condition. Researchers at Stanford University have done a lot of investigations on OPO with 1D single-period $LiNbO_3$ and made great progresses [67–70]. Later, Powers et al. proposed a superlattice with the fan-out structure to be utilized in OPO, as shown in Fig. 9(b). Since the poling period vary continuously in the fan-out superlattice, stable OPO with a wide tunable range can be carried out by adjusting the relative position of the pump light and the NPC [63]. For the sake of the adaption to modern laser technology, improving the tuning range, output energy and conversion efficiency of OPO constantly is the ultimate research goal of this technique.

Terahertz wave is an electromagnetic wave with a frequency band between microwave and light wave. The characteristics of broad bandwidth, high signal-to-noise

1) Adapted with permission from Ref. [62], © The Optical Society

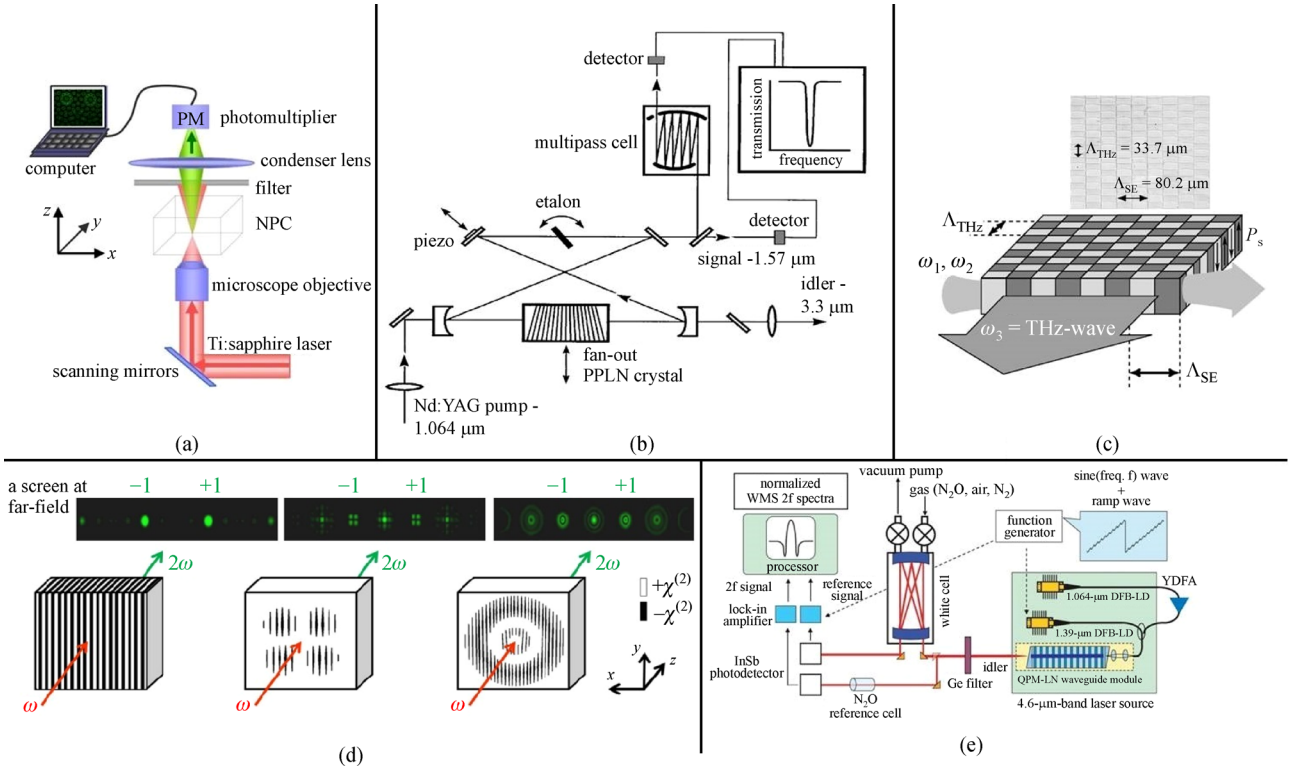

Fig. 9 Experimental schematic of different applications of nonlinear photonic crystal. (a) Domain visualization [9][1]; (b) optical parametric oscillator [63][2]; (c) terahertz-wave difference-frequency generation [64][3]; (d) holographic beam shaping [65]; (e) gas detection [66]

ratio and strong penetrability enable its inestimable values in high-speed wireless mobile communication, military radar and security detection. The principle of terahertz-wave generation based on optical method is the DFG between two laser beams with close wavelengths. Although the conversion efficiency is not as high as that of electrical method, it is possible to generate broadband wave above 1 THz with better coherence [71]. Ito et al. performed a surface-emitted terahertz-wave DFG scheme using a 2D rectangular poled $LiNbO_3$ to avoid the large absorption loss of the nonlinear optical medium in the terahertz region, as shown in Fig. 9(c). In the experiment, the terahertz wave propagates along the direction perpendicular to the incident wave, which reduces its propagation distance within the nonlinear medium, thereby reducing the total absorption loss. Not only can the phase-matching condition on the incident light direction be satisfied, but the phase matching on the terahertz-wave direction is realized by the RLVs in 2D rectangular superlattice. As a result of that, an enhanced tunable 1.5 – 1.8 THz wave with a bandwidth of 10 GHz outputs. It is also suggested that the forward and backward terahertz waves generated simultaneously are possible for higher output power by reflecting one side of that on to the other side [64].

It is also a challenging subject to realize the modulation of light wavefronts by various artificial superlattices. With the rapid development of imaging technology today, an emerging technology of holographic imaging has attracted more and more attention from scientific researchers. In conventional holography, information of an object is stored in a light-sensitive medium, by recording the interference pattern between a reference beam and a beam reflected from the object. This information can later be restored and the object will be reconstructed by illuminating this recording with a reference beam, which is similar to encoding and decoding. After the evolution of more than ten years, the light wavefronts modulation technology is combined with the popular technology of nowadays to develop a more universal technology — nonlinear optical holography [65,72]. The core principle of the technology is to use the actual FW and the imaginary nonlinear polarization wave to interfere with each other for the generation of a nonlinear holographic superlattice. As shown in Fig. 9(d), a quantity of functions such as beam

1) Adapted with permission from Ref. [9], © The Optical Society
2) Adapted with permission from Ref. [63], © The Optical Society
3) Adapted with permission from Ref. [64], © The Optical Society

shaping, free-space imaging of nonlinear light waves can be realized successfully, which provides a new means for the manual adjustment of the physical system based on wave theory.

In the meantime, Japanese researchers designed a real-time N_2O gas detection system for agricultural production using a 4.6-μm-band laser source based on a PPLN ridge waveguide [66], as shown in Fig. 9(e). The relationship between the concentrations of N_2O gas in the air and the content of nitrogen fertilizer in plants can be obtained by the device to reasonably control the amount of nitrogen compounds in soil and reduce the emissions of greenhouse gas, as well as to evaluate whether the soil is environmentally safe for planting. Because N_2O exhibits its strongest absorption band in the 4.6 μm region, a 4.6-μm-band mid-infrared CW laser source is generated by DFG in QPM $LiNbO_3$ crystal on this device. Equipped with the gas sampling, filtering and other modules in the system, the highly sensitive long-term monitoring of N_2O gas is realized. Since the sampled gas contains a huge amount of moisture originating from plant transpiration and the electronic devices are susceptible to moisture damage, the NPC-based scheme avoids this drawback and has extremely high practical application value.

6 Conclusions

From the initial 1D superlattices and the 2D superlattices with many related research results to the 3D superlattices that is currently being explored, there are still numerous novel structures in the nature, such as the microscopic distribution of cells, the geometric distribution in the art of paper-cutting, the topological structure like Mobius ring or the shape of a snowflake to be investigated. It is noteworthy that the snowflake structures are widely found with diverse forms and they have rotational and translational symmetry as well as self-similarity in common. Owing to the wonderful distribution of RLVs corresponding to the three characteristics, the multi-angle and multi-wavelength QPM and ND harmonic generation with high efficiency is likely to be realized if the snowflake structure can be utilized in the design of NPCs. In conclusion, a lot of research directions for NPCs including the exploration of structures, crystal preparation methods and many other aspects are still waiting for cultivation.

Acknowledgements The work was supported by the Fundamental Research Funds for the Central Universities (No. 2018CUCTJ043).

References

1. Armstrong J A, Bloembergen N, Ducuing J, Pershan P S. Interactions between light waves in a nonlinear dielectric. Physical Review, 1962, 127(6): 1918–1939
2. Yamada M, Nada N, Saitoh M, Watanabe K. First-order quasi-phase matched $LiNbO_3$ waveguide periodically poled by applying an external field for efficient blue second harmonic generation. Applied Physics Letters, 1993, 62(5): 435–436
3. Zhu S, Zhu Y, Qin Y, Wang H, Ge C, Ming N. Experimental realization of second harmonic generation in a Fibonacci optical superlattice of $LiTaO_3$. Physical Review Letters, 1997, 78(14): 2752–2755
4. Zhu S, Zhu Y, Ming N. Quasi-phase-matched third-harmonic generation in a quasi-periodic optical superlattice. Science, 1997, 278(5339): 843–846
5. Berger V. Nonlinear photonic crystals. Physical Review Letters, 1998, 81(19): 4136–4139
6. Broderick N G, Ross G W, Offerhaus H L, Richardson D J, Hanna D C. Hexagonally poled lithium niobate: a two-dimensional nonlinear photonic crystal. Physical Review Letters, 2000, 84(19): 4345–4348
7. Fragemann A, Pasiskevicius V, Laurell F. Second-order nonlinearities in the domain walls of periodically poled $KTiOPO_4$. Applied Physics Letters, 2004, 85(3): 375–377
8. Saltiel S M, Neshev D N, Krolikowski W, Arie A, Kivshar Y S. Frequency doubling by nonlinear diffraction in nonlinear photonic crystals. In: Proceedings of International Conference on Transparent Optical Networks. IEEE, 2009, paper Tu.B1.2
9. Sheng Y, Best A, Butt H J, Krolikowski W, Arie A, Koynov K. Three-dimensional ferroelectric domain visualization by Cerenkov-type second harmonic generation. Optics Express, 2010, 18(16): 16539–16545
10. Li H, Mu S, Xu P, Zhong M, Chen C, Hu X, Cui W, Zhu S. Multicolor Čerenkov conical beams generation by cascaded-$\chi^{(2)}$ processes in radially poled nonlinear photonic crystals. Applied Physics Letters, 2012, 100(10): 101101
11. Ma B, Kafka K, Chowdhury E. Fourth-harmonic generation via nonlinear diffraction in a 2D $LiNbO_3$ nonlinear photonic crystal from mid-IR ultrashort pulses. Chinese Optics Letters, 2017, 15(5): 051901
12. Liu S, Switkowski K, Chen X, Xu T, Krolikowski W, Sheng Y. Broadband enhancement of Čerenkov second harmonic generation in a sunflower spiral nonlinear photonic crystal. Optics Express, 2018, 26(7): 8628–8633
13. Sheng Y, Wang W, Shiloh R, Roppo V, Kong Y, Arie A, Krolikowski W. Čerenkov third-harmonic generation in $\chi^{(2)}$ nonlinear photonic crystal. Applied Physics Letters, 2011, 98(24): 241114
14. Yao J, Li G, Xu J, Zhang G. New development of quasi-phase-matching technique. Chinese Journal of Quantum Electronics, 1999, 16(4): 289–294
15. Thomas J, Hilbert V, Geiss R, Pertsch T, Tünnermann A, Nolte S. Quasi phase matching in femtosecond pulse volume structured *x*-cut lithium niobate. Laser & Photonics Reviews, 2013, 7(3): L17–L20
16. Rosenman G, Urenski P, Agronin A, Rosenwaks Y, Molotskii M. Submicron ferroelectric domain structures tailored by high-voltage scanning probe microscopy. Applied Physics Letters, 2003, 82(1): 103–105
17. Yamada M, Kishima K. Fabrication of periodically reversed domainstructure for SHG in $LiNbO_3$ by direct electron beam lithography at room temperature. Electronics Letters, 1991, 27(10): 828–829

18. Wei D, Zhu Y, Zhong W, Cui G, Wang H, He Y, Zhang Y, Lu Y, Xiao M. Directly generating orbital angular momentum in second-harmonic waves with a spirally poled nonlinear photonic crystal. Applied Physics Letters, 2017, 110(26): 261104
19. Magel G A, Fejer M M, Byer R L. Quasi-phase-matched second-harmonic generation of blue light in periodically poled $LiNbO_3$. Applied Physics Letters, 1990, 56(2): 108–110
20. Xu T, Lu D, Yu H, Zhang H, Zhang Y, Wang J. A naturally grown three-dimensional nonlinear photonic crystal. Applied Physics Letters, 2016, 108(5): 051907
21. Leng H. Manipulation of second harmonic waves and entangled photons using two- and three-dimensional nonlinear photonic crystals. Dissertation for the Doctoral Degree. Nanjing: Nanjing University, 2014, 77–79
22. Fejer M M. Nonlinear optical frequency conversion. Physics Today, 1994, 47(5): 25–32
23. Freund I. Nonlinear diffraction. Physical Review Letters, 1968, 21(19): 1404–1406
24. Kalinowski K, Roedig P, Sheng Y, Ayoub M, Imbrock J, Denz C, Krolikowski W. Enhanced Čerenkov second-harmonic emission in nonlinear photonic structures. Optics Letters, 2012, 37(11): 1832–1834
25. Vyunishev A M, Slabko V V, Baturin I S, Akhmatkhanov A R, Shur V Y. Nonlinear Raman-Nath diffraction of femtosecond laser pulses. Optics Letters, 2014, 39(14): 4231–4234
26. Wang X, Zhao X, Zheng Y, Chen X. Theoretical study on second-harmonic generation in two-dimensional nonlinear photonic crystals. Applied Optics, 2017, 56(3): 750–754
27. Miller G D, Batchko R G, Tulloch W M, Weise D R, Fejer M M, Byer R L. 42%-efficient single-pass CW second-harmonic generation in periodically poled lithium niobate. Optics Letters, 1997, 22(24): 1834–1836
28. Saltiel S M, Neshev D N, Krolikowski W, Arie A, Bang O, Kivshar Y S. Multiorder nonlinear diffraction in frequency doubling processes. Optics Letters, 2009, 34(6): 848–850
29. Liu H, Li J, Zhao X, Zheng Y, Chen X. Nonlinear Raman-Nath second harmonic generation with structured fundamental wave. Optics Express, 2016, 24(14): 15666–15671
30. Li H, Fan Y, Xu P, Zhu S, Lu P, Gao Z, Wang H, Zhu Y, Ming N, He J L. 530-mW quasi-white-light generation using all-solid-state laser technique. Journal of Applied Physics, 2004, 96(12): 7756–7758
31. Chen B, Ren M, Liu R, Zhang C, Sheng Y, Ma B, Li Z. Simultaneous broadband generation of second and third harmonics from chirped nonlinear photonic crystals. Light, Science & Applications, 2014, 3(7): e189
32. Wang W, Niu X, Zhou C. Study on broadband second harmonic generation in short-range ordered quadratic medium. Journal of Synthetic Crystals, 2014, 43(5): 1252–1256
33. Gu B, Dong B, Zhang Y, Yang G. Enhanced harmonic generation in aperiodic optical superlattices. Applied Physics Letters, 1999, 75(15): 2175–2177
34. Segal N, Keren-Zur S, Hendler N, Ellenbogen T. Controlling light with metamaterial-based nonlinear photonic crystals. Nature Photonics, 2015, 9(3): 180–184
35. Reyes Gómez F, Porras-Montenegro N, Oliveira O N Jr, Mejía-Salazar J R. Giant second-harmonic generation in cantor-like metamaterial photonic superlattices. ACS Omega, 2018, 3(12): 17922–17927
36. Gómez F R, Porras-Montenegro N, Oliveira O N, Mejía-Salazar J R. Second harmonic generation in the plasmon-polariton gap of quasiperiodic metamaterial photonic superlattices. Physical Review B, 2018, 98(7): 075406
37. Gómez F R, Mejía-Salazar J R. Bulk plasmon-polariton gap solitons in defective metamaterial photonic superlattices. Optics Letters, 2015, 40(21): 5034–5037
38. Robles-Uriza A X, Gómez F R, Mejía-Salazar J R. Multiple omnidirectional defect modes and nonlinear magnetic-field effects in metamaterial photonic superlattices with a polaritonic defect. Superlattices and Microstructures, 2016, 97: 110–115
39. Gómez F R, Mejía-Salazar J R, Oliveira O N, Porras-Montenegro N. Defect mode in the bulk plasmon-polariton gap for giant enhancement of second harmonic generation. Physical Review B, 2017, 96(7): 075429
40. Kasimov D, Arie A, Winebrand E, Rosenman G, Bruner A, Shaier P, Eger D. Annular symmetry nonlinear frequency converters. Optics Express, 2006, 14(20): 9371–9376
41. Qin Y Q, Zhang C, Zhu Y Y, Hu X P, Zhao G. Wave-front engineering by Huygens-Fresnel principle for nonlinear optical interactions in domain engineered structures. Physical Review Letters, 2008, 100(6): 063902
42. Chen B, Zhang C, Liu R, Li Z. Multi-direction high-efficiency second harmonic generation in ellipse structure nonlinear photonic crystals. Applied Physics Letters, 2014, 105(15): 151106
43. Ma B, Wang T, Sheng Y, Ni P, Wang Y, Cheng B, Zhang D. Quasiphase matched harmonic generation in a two-dimensional octagonal photonic superlattice. Applied Physics Letters, 2005, 87(25): 251103
44. Ma B, Ren M, Ma D, Li Z. Multiple second-harmonic waves in a nonlinear photonic crystal with fractal structure. Applied Physics B, Lasers and Optics, 2013, 111(2): 183–187
45. Zhang Y, Gao Z D, Qi Z, Zhu S N, Ming N B. Nonlinear Cerenkov radiation in nonlinear photonic crystal waveguides. Physical Review Letters, 2008, 100(16): 163904
46. Ni P, Ma B, Wang X, Cheng B, Zhang D. Second-harmonic generation in two-dimensional periodically poled lithium niobate using second-order quasiphase matching. Applied Physics Letters, 2003, 82(24): 4230–4232
47. Peng L, Hsu C, Ng J, Kung A. Wavelength tunability of second-harmonic generation from two-dimensional $\chi^{(2)}$ nonlinear photonic crystals with a tetragonal lattice structure. Applied Physics Letters, 2004, 84(17): 3250–3252
48. Ni P, Ma B, Feng S, Cheng B, Zhang D. Multiple-wavelength second-harmonic generations in a two-dimensional periodically poled lithium niobate. Optics Communications, 2004, 233(1–3): 199–203
49. Saltiel S M, Sheng Y, Voloch-Bloch N, Neshev D N, Krolikowski W, Arie A, Koynov K, Kivshar Y S. Cerenkov-type second-harmonic generation in two-dimensional nonlinear photonic structures. IEEE Journal of Quantum Electronics, 2009, 45(11): 1465–1472
50. Wang T, Ma B, Sheng Y, Ni P, Cheng B, Zhang D. Large angle

acceptance of quasi-phase-matched second harmonic generation in a homocentrically poled $LiNbO_3$. Optics Communications, 2005, 252(4–6): 397–401
51. Sheng Y, Koynov K, Zhang D. Collinear second harmonic generation of 20 wavelengths in a single two-dimensional decagonal nonlinear photonic quasi-crystal. Optics Communications, 2009, 282(17): 3602–3606
52. Hou B, Xu G, Wen W, Wong G K. Diffraction by an optical fractal grating. Applied Physics Letters, 2004, 85(25): 6125–6127
53. Park H, Camper A, Kafka K, Ma B, Lai Y H, Blaga C, Agostini P, DiMauro L F, Chowdhury E. High-order harmonic generations in intense MIR fields by cascade three-wave mixing in a fractal-poled $LiNbO_3$ photonic crystal. Optics Letters, 2017, 42(19): 4020–4023
54. Ma B, Li H. High-order nonlinear diffraction harmonics in nonlinear photonic crystals. Chinese Journal of Lasers, 2019, 46(2): 0208001
55. Mateos L, Molina P, Galisteo J, López C, Bausá L E, Ramírez M O. Simultaneous generation of second to fifth harmonic conical beams in a two dimensional nonlinear photonic crystal. Optics Express, 2012, 20(28): 29940–29948
56. Wang W, Sheng Y, Kong Y, Arie A, Krolikowski W. Multiple Čerenkov second-harmonic waves in a two-dimensional nonlinear photonic structure. Optics Letters, 2010, 35(22): 3790–3792
57. Saltiel S M, Neshev D N, Krolikowski W, Voloch-Bloch N, Arie A, Bang O, Kivshar Y S. Nonlinear diffraction from a virtual beam. Physical Review Letters, 2010, 104(8): 083902
58. Vyunishev A M, Arkhipkin V G, Baturin I S, Akhmatkhanov A R, Shur V Y, Chirkin A S. Mutiple nonlinear Bragg diffraction of femtosecond laser pulses in a $\chi^{(2)}$ photonic lattice with hexagonal domains. Laser Physics Letters, 2018, 15(4): 045401
59. Almeida E, Bitton O, Prior Y. Nonlinear metamaterials for holography. Nature Communications, 2016, 7(1): 12533
60. Wei D, Wang C, Wang H, Hu X, Wei D, Fang X, Zhang Y, Wu D, Hu Y, Li J, Zhu S, Xiao M. Experimental demonstration of a three-dimensional lithium niobate nonlinear photonic crystal. Nature Photonics, 2018, 12(10): 596–600
61. Xu T, Switkowski K, Chen X, Liu S, Koynov K, Yu H, Zhang H, Wang J, Sheng Y, Krolikowski W. Three-dimensional nonlinear photonic crystal in ferroelectric barium calcium titanate. Nature Photonics, 2018, 12(10): 591–595
62. Zhang J, Zhao X, Zheng Y, Li H, Chen X. Universal modeling of second-order nonlinear frequency conversion in three-dimensional nonlinear photonic crystals. Optics Express, 2018, 26(12): 15675–15682
63. Powers P E, Kulp T J, Bisson S E. Continuous tuning of a continuous-wave periodically poled lithium niobate optical parametric oscillator by use of a fan-out grating design. Optics Letters, 1998, 23(3): 159–161
64. Sasaki Y, Avetisyan Y, Yokoyama H, Ito H. Surface-emitted terahertz-wave difference-frequency generation in two-dimensional periodically poled lithium niobate. Optics Letters, 2005, 30(21): 2927–2929
65. Shapira A, Naor L, Arie A. Nonlinear optical holograms for spatial and spectral shaping of light waves. Science Bulletin, 2015, 60(16): 1403–1415
66. Tokura A, Asobe M, Enbutsu K, Yoshihara T, Hashida S N, Takenouchi H. Real-time N_2O gas detection system for agricultural production using a 4.6-μm-band laser source based on a periodically poled $LiNbO_3$ ridge waveguide. Sensors (Basel), 2013, 13(8): 9999–10013
67. Myers L E, Miller G D, Eckardt R C, Fejer M M, Byer R L, Bosenberg W R. Quasi-phase-matched 1.064-μm-pumped optical parametric oscillator in bulk periodically poled $LiNbO_3$. Optics Letters, 1995, 20(1): 52–54
68. Myers L E, Bosenberg W R. Periodically poled lithium niobate and quasi-phase-matched optical oarametric oscillators. IEEE Journal of Quantum Electronics, 1997, 33(10): 1663–1672
69. Burr K C, Tang C L, Arbore M A, Fejer M M. High-repetition-rate femtosecond optical parametric oscillator based on periodically poled lithium niobate. Applied Physics Letters, 1997, 70(25): 3341–3343
70. Batchko R G, Weise D R, Plettner T, Miller G D, Fejer M M, Byer R L. Continuous-wave 532-nm-pumped singly resonant optical parametric oscillator based on periodically poled lithium niobate. Optics Letters, 1998, 23(3): 168–170
71. Wang T D, Lin S T, Lin Y Y, Chiang A C, Huang Y C. Forward and backward terahertz-wave difference-frequency generations from periodically poled lithium niobate. Optics Express, 2008, 16(9): 6471–6478
72. Liu H, Zhao X, Li H, Zheng Y, Chen X. Dynamic computer-generated nonlinear optical holograms in a non-collinear second-harmonic generation process. Optics Letters, 2018, 43(14): 3236–3239

Huangjia Li received the bachelor degree of engineering from Communication University of China. She is currently pursuing the master degree in School of Data Science and Media Intelligence, Communication University of China. Her present research work involves the nonlinear photonic crystals with snowflake superlattices and their nonlinear optical properties.

Boqin Ma received the Ph.D. degree from the Institute of Physics, Chinese Academy of Sciences, Beijing, China, in the field of Optics in 2005. Since then, she joined the Faculty of Science and Technology, Communication University of China. In 2011, she received the position of associate professor. She has been working on the nonlinear interactions between nonlinear photonic crystals and laser beams.